12-2016

On the propagation of atmospheric gravity waves in a non-uniform wind field: Introducing a modified acoustic-gravity wave equation

Ahmad Talaei
Utah State University

On the propagation of atmospheric gravity waves in a non-uniform wind field: Introducing a modified acoustic-gravity wave equation

Ahmad Talaei and Michael J. Taylor

Center for Atmospheric and Space Sciences, Department of Physics, Utah State University, Logan, UT

Corresponding author: Ahmad Talaei (ahmad.talaei@gmail.com)

Keywords:

Atmospheric gravity waves, acoustic-gravity wave, Boussinesq approximation, and Taylor-Goldstein equation

Key Points:

- The new mathematical solution introduced in this paper, gives the acoustic-gravity wave equation without the need to Boussinesq approximation which has recognized limitations.
- The resultant wave equation is a significant improvement to the well-known Taylor-Goldstein equation, the starting point for most recent analyses of the effects of wind shear on gravity waves.
- The new term in the amplitude of the vertical velocity of acoustic-gravity waves is introduced which may play a significant role in directional filtering of atmospheric waves in a realistic atmosphere with strong and highly variable winds.

Abstract

Atmospheric gravity waves play fundamental roles in a broad-range of dynamical processes extending throughout the Earth's neutral atmosphere and ionosphere. In this paper, we present a modified form for the acoustic-gravity wave equation and its dispersion relationships for a compressible and non-stationary atmosphere in hydrostatic balance. Importantly, the solutions have been achieved without the use of the well-known Boussinesq approximation which have been used extensively in previous studies.

We utilize the complete set of governing equations for a compressible atmosphere with non-uniform airflows to determine an equation for vertical velocity of possible atmospheric waves. This intricate wave equation is simplified by a proper substitution producing a useful new wave-like equation for acoustic-gravity waves. The substitution introduces a term Ω (intrinsic frequency) in the amplitude of the wave solution for the vertical velocity of acoustic-gravity waves. This term may play a significant role in directional filtering of atmospheric waves in realistic atmospheres exhibiting strong and highly variable winds. It is also proven that the only difference in the wave equation of compressible fluid when non-uniform wind is added to the equations of motion is the term with second derivative of $ln\Omega$ with respect to height. These new solutions may be particularly important for improved gravity wave propagation studies in the upper mesosphere and thermosphere/ionosphere regions.

1 Introduction

Since the seminal work of Hines [Hines, 1960] and colleagues paving the way forward for studying the propagation and impact of gravity waves on the upper atmosphere, there have been many improvements to the basic theory to account wave propagation in a realistic, highly variable 'windy' atmosphere [e.g. Bretherton, 1966; Booker and Bretherton, 1967; Jones, 1968; Hazel, 1972; Turner, 1973; Chimonas, 1974; Gossard and Hooke, 1975; Fua et al., 1976; Lalas and Einaudi, 1976; Fua and Einaudi, 1984; Garratt, 1992; Sutherland et al., 1994; Chimonas, 2002; Drazin, 2002; Teixeira et al., 2004; and Nappo, 2008]. Atmospheric gravity waves (GWs) are now known to play key roles in a broad-range of dynamical processes extending from Earth's surface well into the thermosphere and ionosphere. Due to their observed growth with altitude, and the onset of wave instability and dissipation effects, gravity wave influences are largest in the upper mesosphere [see review by Fritts and Alexander, 2003] and thermosphere/ionosphere regions [see e.g., Vadas and Fritts, 2005; Vadas, 2007; Hocke and Schlegel, 1996]. These waves are excited primarily in the lower atmosphere by strong convection, topography, and wind shears. Indeed, gravity waves are now known to play a global role with the deposition of wave momentum flux forcing closure of the mesospheric jets in the summer and winter hemispheres, and driving a residual meridional inter-hemispheric circulation that results in the remarkably cold summer mesopause at polar latitudes, due to strong adiabatic cooling [e.g., Lindzen, 1973, 1981; Holton, 1982; Garcia and Solomon, 1985]. Improving our knowledge of the basic properties, propagation and dissipation effects of gravity waves within the atmosphere is therefore of high importance. This study returns to the basic gravity wave equation sets and presents a new solution without the need for prior simplifying approximations.

In general, there are two ways to introduce the wave-like equation for gravity waves. The first method uses the equations of motion in an approximation form, termed the "Boussinesq approximation". This approximation assumes that the equation of continuity can be simplified by ignoring compressibility effects. This method with added non-uniform background winds to the

equations of motion in hydrostatic balance, gives rise to the well-known Taylor-Goldstein (TG) equation [e.g. Taylor, 1931; Goldstein, 1931; Gossard and Hooke, 1975; and Nappo, 2008].

The second way is to use the full equation set for a compressible atmosphere which includes both sound waves and gravity waves. When non-uniform background winds are added to the equations of motion in hydrostatic balance, this method produces a complex differential equation (see Eq. (14)). That to date has deterred the determination of a wave-like solution analytically. In this paper, a proper substitution is presented that reduces the intricate terms of the differential equation and then introduces a useful new wave-like equation for acoustic-gravity waves in the presence of non-uniform wind.

The resultant wave equation for compressible atmosphere differs from the TG relation not only because it includes the acoustic term but also because our solution for the wave equation involves the term Ω in the amplitude of the wave solution (where Ω is the intrinsic frequency which is the wave frequency noted by an observer drifting with the background flow). This term may play a significant role in the gravity wave amplitude growth in a highly variable atmosphere, when they propagate opposite to the wind direction.

In section 2, the complete set of governing equations for compressible atmosphere is introduced and then the new wave equation for acoustic-gravity waves is extracted. It is shown that the only difference in the wave equation, with and without the background wind, is a term with a second derivative of $ln\Omega$ with respect to height. This term involves the first and second derivatives of the wind velocity. The limits of the Boussinesq approximation used in the TG equation are discussed in details then.

In section 3, we have compared the vertical wavenumber square m^2 obtained by TG relation with the one obtained in this paper. We have simulated three different distributions to the background wind in isothermal conditions. First, we considered a background wind with a Gaussian distribution moving in the same wave direction. Then, we simulated the background wind profile with the first derivative of a Gaussian function moving in the same wave propagation direction. And finally, we considered a gravity wave propagating in opposite wind direction with a simulated first derivative of a Gaussian distribution for the background wind. It is shown that our equation presents a ducting region where the wind speed is approaching a maximum, and in the either side this region where the wind speed is decreasing in value, it predicts evanescent gravity waves. Indeed, our equation predicts that the peak in the background wind serves the wave energy and allows to carry wave system over great horizontal distance without significant leakage. The conditions for ducting is found to be quite different from the TG relation.

In section 4, the dispersion relationships for acoustic-gravity waves in a moving atmosphere with constant vertical wavenumber is extracted.

2 Governing equations

Following in the footsteps of many prior gravity waves studies we assume that the Earth's atmosphere behaves as an ideal gas and, in the absence of perturbation, is stratified under the influence of gravity. We then consider the wave motion in this stratified and compressible atmosphere with a non-uniform background wind field. We also do not consider the effects of friction, viscosity, rotation and sphericity. It is well explained in the literature that how wave

motion is created in such an atmosphere by a small vertical perturbation of an air parcel. The momentum and mass conservation equations are then:

$$\rho \frac{D\vec{v}}{Dt} = -\vec{\nabla}p + \rho\vec{g} \tag{1}$$

$$\frac{D\rho}{Dt} + \rho\vec{\nabla}\cdot\vec{v} = 0 \tag{2}$$

Where ρ is density, $\vec{v}$ the velocity vector of the air parcel, p the pressure, g the acceleration due to gravity and $\frac{D}{Dt} = \frac{\partial}{\partial t} + \vec{v}\cdot\vec{\nabla}$ a material derivative which represents the wave intrinsic frequency. For a dry ideal gas, the internal energy is a function of temperature $dU = c_v dT$. Then, the first law of thermodynamics in the material derivative form becomes:

$$c_v \frac{DT}{Dt} + p\frac{DV}{Dt} = \dot{Q} \tag{3}$$

Where c_p is the specific heat capacity at constant pressure, V the specific volume (inverse density) and $\dot{Q}$ the rate of energy input per unit mass (in general with possible contributions from thermal diffusion, conductivity, viscous heating, radiative heating etc.). Eq. (3) is indeed a differential form of the first law of thermodynamics. Now, using the mass continuity equation, Eq. (3) takes the form:

$$c_v \frac{DT}{Dt} + \frac{p}{\rho}\vec{\nabla}\cdot\vec{v} = \dot{Q} \tag{4}$$

Alternatively, using the ideal gas equation $p = \rho RT$, one may eliminate T in favor of p as:

$$\frac{Dp}{Dt} + \gamma p\vec{\nabla}\cdot\vec{v} = \dot{Q}\frac{\rho R}{c_v} \tag{5}$$

Where R is the mean molecular weight of the gas and $\gamma = \frac{c_p}{c_v}$ is the heat capacity ratio. The later thermodynamic equation (Eq. 5) in combination with mass conservation equation (Eq. (2)) for an adiabatic process gives $\frac{Dp}{Dt} = c^2\frac{D\rho}{Dt}$ where c is the local speed of sound. This is a well-known equation that states that in a reversible process the rate of change of pressure of an air parcel is equal to the square of sound speed times the corresponding rate of change of density. This thermodynamic equation represents the principle of conservation of energy, and in fluids in which the equation of state involves temperature the thermodynamic equation is necessary to obtain a closed system of equations.

In order to distinguish between background fluid properties and wave induced properties we use the subscript 0 to designate the background fluid properties and subscript 1 to perturbed fluid properties associated with the wave. All of the local fluid variables are linearized with background states and perturbation variable as:

$$\begin{aligned} u(x,z,t) &= u_0(z) + u_1(x,z,t) \\ \mathrm{w}(x,z,t) &= w_1(x,z,t) \\ \rho(x,z,t) &= \rho_0(z) + \rho_1(x,z,t) \\ p(x,z,t) &= p_0(z) + p_1(x,z,t) \end{aligned} \tag{6}$$

We have used a two-dimensional (x, z) reference plane where x lies in horizontal direction and z represents altitude. The velocities in the x and z directions are u and w. To simplify the analysis we exclude dependence on the y direction but note that waves with any direction of horizontal propagation could be written in the x direction by suitable choice of the x axis. It is assumed that the background states are known and only a function of height, namely an atmosphere whose properties vary only in the z direction. This is one of the basic assumptions which is frequently used for studying the Earth's atmosphere but it has consequences e.g. it ignores horizontal wind shear effects. The vertical component of the background wind $w_0(z)$ is considered to be zero because in the vertical direction, they are almost negligible compared to their horizontal components. We also assume that the perturbations are much smaller than background components so they do not affect the background state. Therefore, the products of the perturbations can be neglected with respect to background-perturbation products. Moreover, we assume that the background state is in hydrostatic balance. This is one of the most fundamental balances in geophysical fluid dynamics and for large scale flows (wavelength >1 km) in the atmosphere, the conceptual simplifications afforded by this approximation can hardly be overemphasized [e.g. Vallis, 2006]. It is, indeed, a consequence of our initial assumption that the background fluid is static vertically $(w_0(z) = 0)$. Therefore, the momentum in z direction leads to:

$$\frac{dp_0}{dz} \approx -\rho_0 g \tag{7}$$

This shows that the pressure term is the only one which can balance the gravitational term. p_0 is only a function of variable z so its derivative with respect to z is denoted by $\frac{d}{dz}$. Now, the momentum equation in the x direction, the momentum equation in the z direction, the equation of continuity and the thermodynamic equation for no heat conduction $(\dot{Q} = 0)$ together with linearized variables and background flow under hydrostatic balance take the following forms, respectively:

$$\frac{\partial u_1}{\partial t} + u_0 \frac{\partial u_1}{\partial x} + w_1 \frac{du_0}{dz} = -\frac{1}{\rho_0} \frac{\partial p_1}{\partial x} \tag{8}$$

$$\frac{\partial w_1}{\partial t} + u_0 \frac{\partial w_1}{\partial x} + \frac{\rho_1}{\rho_0} g = -\frac{1}{\rho_0} \frac{\partial p_1}{\partial z} \tag{9}$$

$$\frac{\partial \rho_1}{\partial t} + u_0 \frac{\partial \rho_1}{\partial x} + w_1 \frac{d\rho_0}{dz} = -\rho_0 \left(\frac{\partial u_1}{\partial x} + \frac{\partial w_1}{\partial z} \right) \tag{10}$$

$$\frac{\partial p_1}{\partial t} + u_0 \frac{\partial p_1}{\partial x} + w_1 \frac{dp_0}{dz} = -\gamma p_0 \left(\frac{\partial u_1}{\partial x} + \frac{\partial w_1}{\partial z} \right) \tag{11}$$

These are the governing equations used for analyzing the gravity waves in a compressible atmosphere with non-uniform background wind. Now, differentiating the momentum equation in the x direction with respect to time, and using the thermodynamic equation under hydrostatic balance leads to (see Appendix A):

$$\frac{\partial^2 u_1}{\partial t^2} + \left({u_0}^2 - \frac{\gamma p_0}{\rho_0}\right)\frac{\partial^2 u_1}{\partial x^2} + 2u_0\frac{\partial^2 u_1}{\partial t \partial x} = \left[\left(-u_0\frac{du_0}{dz} - g + \frac{\gamma p_0}{\rho_0}\frac{\partial}{\partial z}\right)\frac{\partial}{\partial x} - \frac{du_0}{dz}\frac{\partial}{\partial t}\right] w_1 \quad (12)$$

Similarly, differentiating the momentum equation in the z direction with respect to time, and using the thermodynamic equation, the momentum equations in the x direction and the equation of continuity again under hydrostatic balance leads to (see appendix A):

$$\frac{\partial^2 w_1}{\partial t^2} + {u_0}^2\frac{\partial^2 w_1}{\partial x^2} - \frac{\gamma p_0}{\rho_0}\frac{\partial^2 w_1}{\partial z^2} + 2u_0\frac{\partial^2 w_1}{\partial t \partial x} + \gamma g\frac{\partial w_1}{\partial z} + w_1\left(\frac{du_0}{dz}\right)^2 = \left[\left(-u_0\frac{du_0}{dz} - (\gamma - 1)g + \frac{\gamma p_0}{\rho_0}\frac{\partial}{\partial z}\right)\frac{\partial}{\partial x} - \frac{du_0}{dz}\frac{\partial}{\partial t}\right] u_1 \quad (13)$$

We may use $c_s^2(z) = \gamma RT = \frac{\gamma p_0}{\rho_0}$ as the square of the speed of sound which is a function of temperature and the temperature itself is a function of height. We now, multiply $\left(\frac{\partial^2}{\partial t^2} + ({u_0}^2 - c_s^2)\frac{\partial^2}{\partial x^2} + 2u_0\frac{\partial^2}{\partial t \partial x}\right)$ to Eq.

(13) and then use Eq. (12) to cancel u_1 in favor of w_1 knowing that the variables inside the brackets in the right hand side of Eqs. (12) and

(13) are not functions of x and t. Then after some cancelation, Eq.

(13) becomes only a function of w_1 as (see appendix A):

$$\begin{aligned}
&\frac{\partial^2}{\partial t^2}\left[\frac{1}{c_s^2}\frac{\partial^2 w_1}{\partial t^2} + \left(\frac{6{u_0}^2}{c_s^2} - 1\right)\frac{\partial^2 w_1}{\partial x^2} - \frac{\partial^2 w_1}{\partial z^2} + \frac{\gamma g}{c_s^2}\frac{\partial w_1}{\partial z}\right] + \\
&2u_0\frac{\partial^2}{\partial t \partial x}\left[\frac{2}{c_s^2}\frac{\partial^2 w_1}{\partial t^2} + \left(\frac{2{u_0}^2}{c_s^2} - 1\right)\frac{\partial^2 w_1}{\partial x^2} - \frac{\partial^2 w_1}{\partial z^2} + \left(\frac{\gamma g}{c_s^2} + \frac{1}{u_0}\frac{du_0}{dz}\right)\frac{\partial w_1}{\partial z}\right. \\
&\qquad \left. - \frac{\gamma g}{2c_s^2}\left(\frac{1}{u_0}\frac{du_0}{dz}\right)w_1\right] + \\
&{u_0}^2\frac{\partial^2}{\partial x^2}\left[\left(\frac{{u_0}^2}{c_s^2} - 1\right)\frac{\partial^2 w_1}{\partial x^2} - \frac{\partial^2 w_1}{\partial z^2} + \left(\frac{\gamma g}{c_s^2} + \frac{2}{u_0}\frac{du_0}{dz}\right)\frac{\partial w_1}{\partial z}\right. \\
&\qquad \left. - \left(\frac{\gamma g}{c_s^2}\left(\frac{1}{u_0}\frac{du_0}{dz}\right) + \left(\frac{1}{u_0}\frac{du_0}{dz}\right)^2 + \frac{(\gamma - 1)g^2}{{u_0}^2 c_s^2}\right)w_1\right] = 0
\end{aligned} \quad (14)$$

Although this forth-order partial differential equation with three variables seems superficially complicated, all the terms with single z derivative are eliminated if we seek a plane-wave like solution of the form $w_1 = \widetilde{w}_1(z)\cdot(\omega - u_0(z)k)\cdot e^{i(kx-\omega t)+\left(\frac{\gamma g}{2c_s^2}\right)z}$ with constant speed of sound. Indeed, we look for a solution that assumes the vertical perturbation velocity behaves as a plane-wave moving in the x direction with a constant frequency ω and a constant horizontal wavenumber k. However, its amplitude is a function of z and possesses an exponential increase

with height. The perturbation velocity could behave as a plane-wave moving in z direction, as well, if $\widetilde{w}_1(z)$ consists of e^{imz} with constant vertical wavenumber of m. Note that the units of $\widetilde{w}_1(z)$ are meters.

The term $(\omega - u_0 k) \cdot e^{\left(\frac{\gamma g}{2c_s^2}\right)z}$ in the substitution comes from the exponential of the integral of $\frac{\gamma g}{2c_s^2} - \frac{k}{\Omega}\frac{du_0}{dz}$ along the wave's propagation trajectory through the structured atmosphere namely the accumulation effects of the terms multiplied to $\frac{\partial w_1}{\partial z}$ in Eq. (14). After some mathematical developments, Eq. (14) with the given wave like solution results in the following simplified form for $\widetilde{w}_1(z)$:

$$\frac{d^2\widetilde{w}_1}{dz^2} + \left[\frac{(\gamma-1)g^2}{\left(\frac{\omega}{k}-u_0\right)^2 c_s^2} + \frac{(\omega - u_0 k)^2}{c_s^2} - \frac{\left(\frac{du_0}{dz}\right)^2}{\left(\frac{\omega}{k}-u_0\right)^2} - \frac{\frac{d^2u_0}{dz^2}}{\left(\frac{\omega}{k}-u_0\right)} - \left(\frac{\gamma g}{2c_s^2}\right)^2 - k^2\right]\widetilde{w}_1 = 0 \qquad (15)$$

All the terms inside the bracket can be replaced by $m^2(z)$. With no background wind (stationary atmosphere), Eq. (15) reduces to the same equation presented in the literature by initially considering the compressibility [e.g., Hines, 1960; and Vallis, 2006]. The first term inside the bracket $\frac{(\gamma-1)g^2}{c_s^2}$ in Eq. (15) is the buoyancy term. It can be replaced by $\frac{g\kappa}{H_s}$ where the scale height is defined as $H_s = \frac{RT}{g} = \frac{c_s^2}{\gamma g}$ and $\kappa = \frac{R}{c_p} = \frac{\gamma-1}{\gamma}$. For an isothermal atmosphere, this term becomes the Brunt-Väisälä frequency N^2 (the general form of Brunt-Väisälä frequency comes from $N^2 = \frac{(\gamma-1)g^2}{c_s^2} + \frac{g}{T_0}\frac{dT_0}{dz}$ where the positive $\frac{dT_0}{dz}$ increases the buoyancy in the atmosphere, e.g. in stratosphere and negative decreases the buoyancy, e.g. in the troposphere and mesosphere). The second term is related to sound waves and is a function of z. It is because of this term that Eq. (15) gives the wave equation for acoustic waves, as well. For gravity waves with the horizontal phase speed of $\left(c_p - u_0\right)^2 \ll c_s^2$, this term can be ignored in order to study pure gravity waves. The third and fourth terms are due to the non-uniform wind field and both can be replaced by $\frac{d^2}{dz^2} ln\Omega$. The fifth term inside the bracket can be replaced by the term $\frac{1}{4H_s^2}$ where the scale height is a function of temperature and becomes constant in isothermal atmosphere. Eq. (15) is called acoustic-gravity wave equation and gives the exact solution for $\widetilde{w}_1(z)$. The solution for the vertical wave velocity then comes from $w_1(x,z,t) = \widetilde{w}_1(z) \cdot \Omega \cdot e^{i(kx-\omega t)+\frac{z}{2H_s}}$. Once we have the solution for $w_1(x,z,t)$, we can find all the other variables u_1, ρ_1 and p_1 from Eqs. (12), (9) and (8), respectively.

The resultant wave equation for compressible atmosphere differs from the TG equation, the wave equation extracted using the Boussinesq approximation, not only because it includes the acoustic term but also because our solution for the wave equation involves the term Ω in the amplitude of the wave solution.

The Boussinesq approximation exploits a set of governing equations using only small density variations in a fluid. This significantly simplifies math involved with the set of motion equations. However, this approximation which assumes no change in fluid density (except when

multiplied to gravity acceleration in momentum equation) is not valid for Earth atmosphere in *large* scale. In atmosphere, the density varies significantly in the vertical direction as it reduces by large factors without limit. Therefore, the Boussinesq approximation limits to gravity waves with a wavelength much less than the fluid scale height (e.g. for an isothermal atmosphere it requires $kH_s \; or \; mH_s \gg 1$) [see e.g., Lighthill, 1978; Vallis, 2006; and Nappo, 2008].

If we consider the fluid incompressible ($\delta\rho/\rho \ll 1$) with a basic calculation for an ideal fluid (no viscosity effect) in a steady state, one can show that this incompressibility is satisfied only when fluid velocity is low in comparison with the speed of sound in the fluid $\delta\rho/\rho \approx v^2/c_s^2$ [see e.g. Levich, 1962]. In the other words, the Boussinesq approximation should be used for the fluids with velocities much less than the speed of the sound waves. Therefore, the conditions under which incompressibility is a good approximation to the equation of continuity depends not only on the physical nature of the fluid but also on the flow itself.

The upper atmosphere is very irregular as it contains non-uniform horizontal winds with velocities that vary in magnitude and direction continuously [see e.g., Liller and Whipple, 1954]. The typical values of atmosphere wind velocity u_0 and horizontal phase speed of gravity waves c_p below 100 km altitude are usually less than 100 m/s still much less than the speed of sound. The typical interested range of gravity wavelengths are 5-200 km and the typical scale height in mesosphere is around 5-6 km. Now, the typical range of data proves that the condition $kH_s \; or \; mH_s \gg 1$ is satisfied only for shorter wavelength gravity waves with nearly λ_x or $\lambda_z <$ 20 km and the Boussinesq approximation (i.e. incompressibility) is not valid in scales larger than that.

Eq. (15) is extracted for a compressible fluid so it includes the possible presence of sound waves as well as gravity waves. Like the TG relation, it is limited to an isothermal atmosphere, due to the constant speed of sound assumption. However, in its wave solution, the amplitude of the wave vertical velocity includes an additional term Ω, that is not present in the TG equation solution.

3 Vertical wavenumber comparison

In this section, we have compared the vertical wavenumber squared, given by Taylor-Goldstein relation (e.g. Eq. 2.42, Nappo, 2014) with the one given herein by Eq. (15). To do this, we have considered three different distributions to the background wind in an isothermal atmosphere. For the first simulated case, we considered a background wind with a Gaussian distribution moving in the same direction as the wave. We then simulated the background wind given by the first derivative of a Gaussian function and again moving in the same wave propagation direction. Finally, we considered a gravity wave propagating in opposite wind directions with a background wind distribution simulated by first derivative of the Gaussian function. For these comparisons, we have considered an isothermal atmosphere from 80 to 100 km altitude and assumed $N^2 = 5.5 \cdot 10^{-4}\; s^{-2}$, the speed of sound $c_s = 270\; m/s$ and scale height $H_s = 5.5\; km$, all appropriate to this region of the atmosphere. The range of horizontal wavelengths was varied from 10 to 100 km. The selected gravity wave observed periods were 5, 10, 20 and 30 min. The waves of interest here are such that $c_p > u_0$ so no critical levels in the Doppler-shifted intrinsic frequency are involved.

3.1 Background wind with Gaussian profile

The first simulated case is a Gaussian distribution for the background wind moving in the direction of wave propagation. Consider the Gaussian distribution in the form of:

$$u_0(z) = U_0 \cdot e^{-\frac{(z-z_0)^2}{2\cdot\sigma^2}} \tag{16}$$

It is assumed that this wind duct is distributed from 80 to 100 km height. The values of $U_0 = 30$, $z_0 = 90\ km$ and $\sigma = 2\ km$ gives a peak of wind velocity of 30 m/s centered at 90 km and the tails with approximately zero velocity.

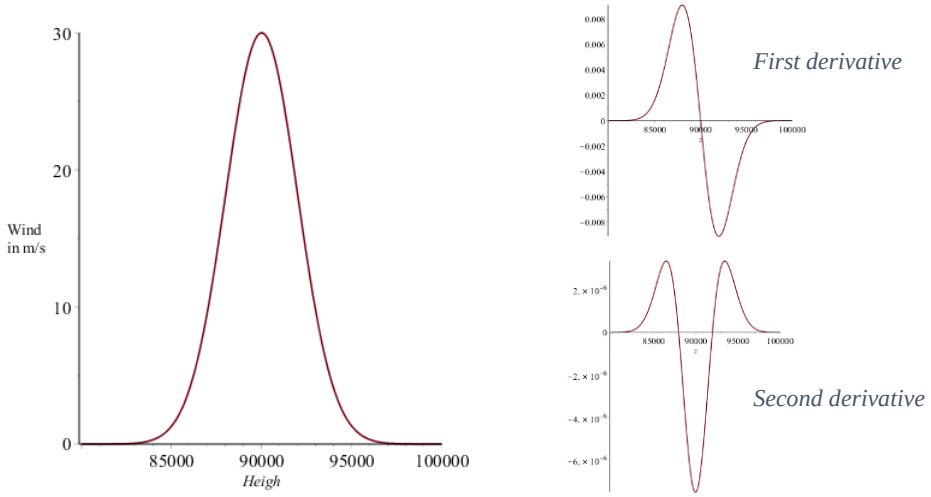

Figure 1. Gaussian background wind profile from 80 to100 km altitude with its first and second derivative profiles.

Figure 2Figure 3 display the contour plots for m^2 for a gravity wave with a 5 min period. The magnitude of m^2 is presented by the coloring contour from Blue to VioletRed. We have considered the following seven different values for m^2as $-1\cdot10^{-8}, -1\cdot10^{-9}, 0, 1\cdot10^{-9}, 1\cdot10^{-8}, 1\cdot10^{-7}$ and $1\cdot10^{-6}$ spanning the vertical wavelength range from about 6 to 200 km. The Blue color represents the smallest $(-1\cdot10^{-8})$ while VioletRed denotes the largest vertical wavenumber square $(1\cdot10^{-6})$. The solid lines in each plot represent $m^2 = 0$ where the transition from positive m^2 to negative occurs. The contour plots in Figure 2 are obtained from Eq. (15) while Figure 3 results from the TG relation. Both plots use the same axes scales for direct comparison.

As is evident, for shorter horizontal wavelengths $(\lambda \leq 15\ km)$, both the TG relation and our new Eq. (15) predict positive m^2 with almost identical vertical wavelengths. However, for horizontal wavelengths longer than 15 km the discrepancies between two figures becomes increasingly evident where the Boussinesq approximation is no longer valid.

For gravity waves with horizontal wavelengths from 15 to 65 km, Eq. (15) gives positive m^2 (real vertical wavenumber) within about 2 km of the location of the maximum of the wind peak, negative m^2 (complex vertical wavenumber) above and below the wind peak (i.e. $z <$ 87 km and $z > 93\ km$) and positive m^2 again in the tails of the wind profile. In comparison, for waves with horizontal wavelengths from 25 to 45 km, the TG relation predicts a negative m^2 within about 2 km of the location of the maximum of the wind peak and positive m^2 above and below.

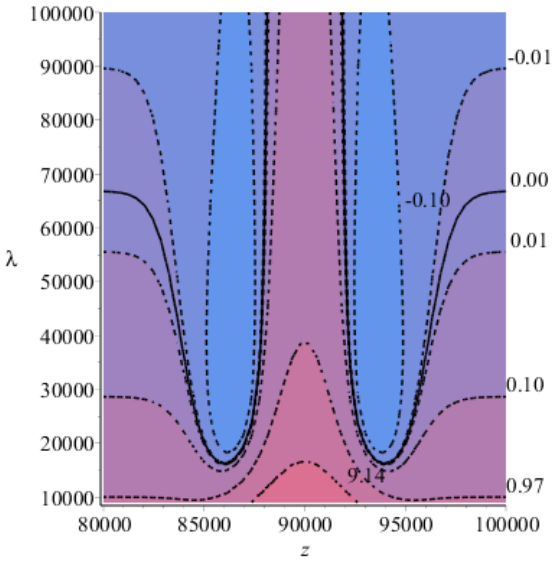

Figure 2. Vertical wavenumber square obtained for a gravity wave with 5 min period and the horizontal wavelength range from 10 to 100 km propagating in an isothermal atmosphere from 80 to 100 km altitude. The m^2 values must be multiplied by 10^{-7}.

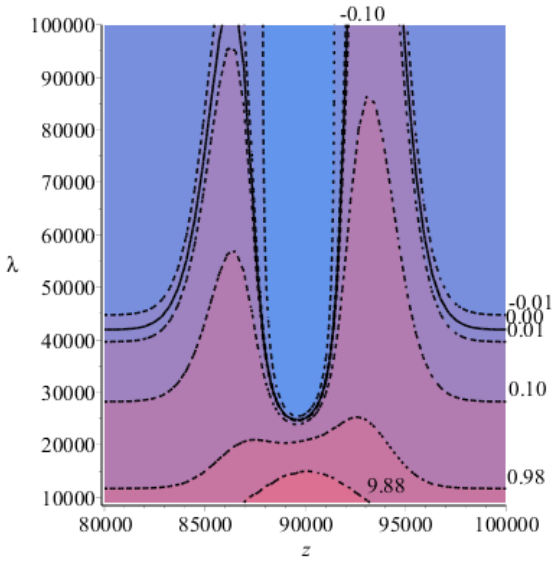

Figure 3. Vertical wavenumber square obtained by TG relation for a gravity wave with 5 min period and horizontal wavelength range from 10 to 100 km propagating in an isothermal atmosphere from 80 to 100 km altitude. The m^2 values must be multiplied by 10^{-7}.

It is well documented in the literature that Doppler ducting can occur whenever the mean profile of wind has a local maximum [see e.g., Chimonas, 1986; Lindzen, 1976; Isler, 1997; and Nappo, 2014]. Indeed, a strong localized peak in the background wind is able to trap the wave energy and allow the wave to propagate over large horizontal distance without significant dissipation [see e.g., Pautet, 2005].

Eq. (15) predicts that longer wavelength gravity waves in the vicinity of the wind maximum remain ducted while the TG relation predicts that such waves would be evanescent. This is because of the dominance of the term with the second derivative of wind velocity in Eq. (15). Indeed, the second derivative of background wind plays a main role in both the TG relation and in Eq. (15). However, in TG relation this term appears with a positive sign and therefore m^2 closely follows the second derivative of wind profile. In Eq. (15), this term is subtractive and so m^2 follows the opposite to the second derivative of wind profiles.

Eq. (15) also predicts that the waves above and below the wind peak become evanescent (i.e. no longer ducted) while the TG relation still indicates propagating conditions for the gravity waves. For gravity waves with longer horizontal wavelengths both figures give negative m^2 in the altitude of tails of the wind profile.

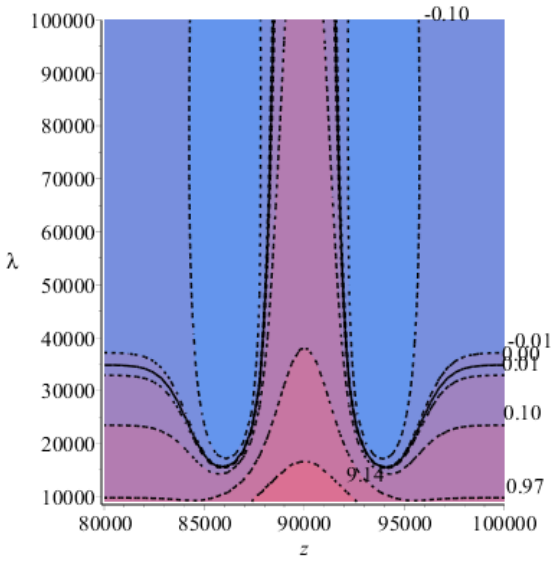

Figure 4. Vertical wavenumber square obtained for a gravity wave with 5 min period without the second term in Eq. 15. The m^2 values must be multiplied by 10^{-7}.

As mentioned before, the second term in Eq. (15) is related to acoustic waves and does not appear in the TG relation. For gravity waves with the horizontal phase speed limit of $\left(c_p - u_0\right)^2 \ll c_s^2$, one can neglect this term as compared with the sixth term, k^2. Ignoring this term gives a wave equation and a solution for a pure gravity waves. This approximation, however, is not equivalent to the Boussinesq approximation as it does not deal with the compressibility of the fluid. Hines called this the 'asymptotic limit' and showed that it is sufficiently accurate for the most pertinent calculations [Hines, 1960]. Keeping the second term and omitting the first one inside the bracket in Eq. (15) provides the wave equation and dispersion relationship for a pure sound wave i.e. waves unaffected by buoyancy. This approximation completely decouples the two types of sound and gravity waves, and assumes that neither is influenced by the presence of the other.

The Figure 4 displays m^2 for the case where the term $\frac{\Omega^2}{c_s^2}$ is ignored in Eq. (15). Comparing this plot with Figure 2, you can see only where the horizontal wavelength becomes longer there are changes in the m^2 profiles. This term only plays a role when the wave period is small and the horizontal wavelength is large which means the wave phase speed increases and the asymptotic limit $\left(c_p - u_0\right)^2 \ll c_s^2$ is not valid any more. For higher wave periods the results with and without this term are almost identical and this term does not play a central role as compared with the term k^2.

The following figures represent the contour plots for m^2 in the same conditions but for a gravity waves with observed periods of 10, 20 and 30 min. For comparison the contour plots for m^2 are the same as the ones in Figures 2 and 3. The primary difference between these longer period results is that the distance between the individual contours has increased significantly and this tends to support waves with larger horizontal scales. This in turn changes the threshold values for horizontal wavelengths where the discrepancy becomes apparent.

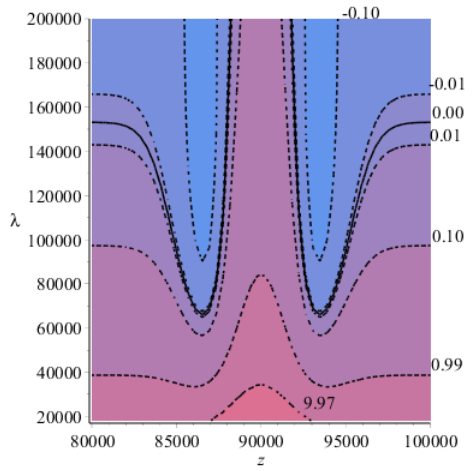

Figure 5. Vertical wavenumber square obtained for a gravity wave with 10 min period.

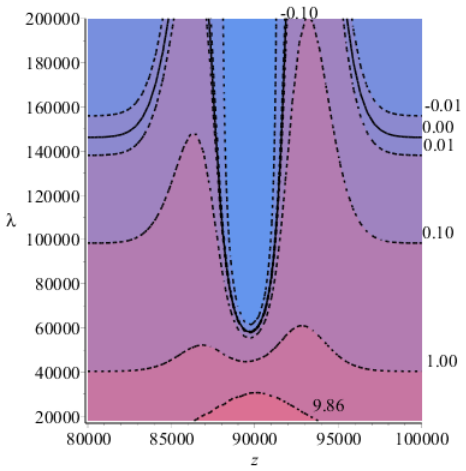

Figure 6. Vertical wavenumber square obtained by TG relation for a gravity wave with 10 min period.

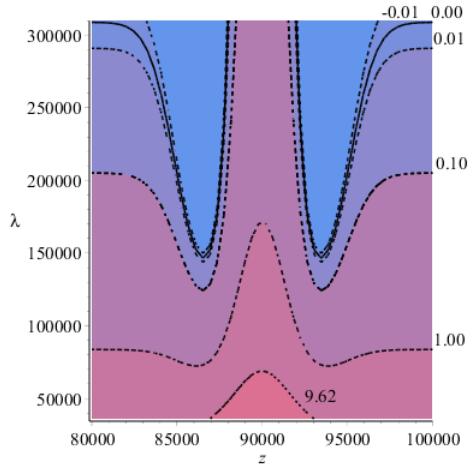

Figure 7. Vertical wavenumber square obtained for a gravity wave with 20 min period.

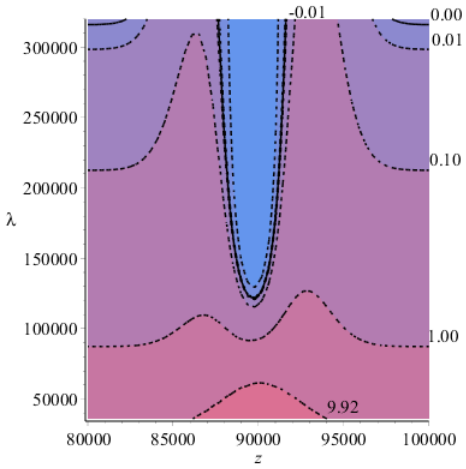

Figure 8. Vertical wavenumber square obtained by TG relation for a gravity wave with 20 min period.

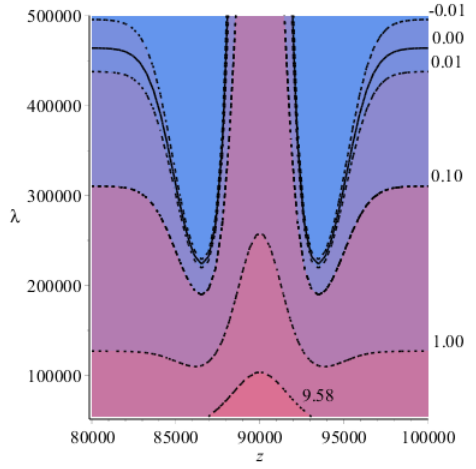

Figure 9. Vertical wavenumber square obtained for a gravity wave with 30 min period.

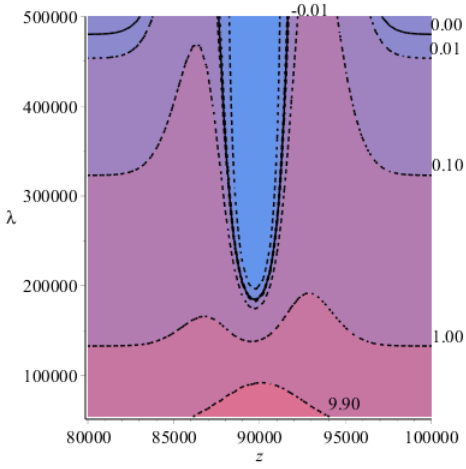

Figure 10. Vertical wavenumber square obtained by TG relation for a gravity wave with 30 min period.

3.2 Background wind with derivative of Gaussian profile

The background wind in upper atmosphere may also have a profile similar to the first derivative of Gaussian distribution and representing a strong shear. Consider a gravity wave propagating in the same direction as the wind with the following distribution:

$$u_0(z) = U_0 + \frac{d}{dz}\left(\alpha \cdot e^{-\frac{(z-z_0)^2}{2\cdot\sigma^2}}\right) \tag{17}$$

With the values of $U_0 = 15$, $\alpha = 4.95\times10^4$, $z_0 = 90\ km$ and $\sigma = 2\ km$, this function gives a maximum of wind velocity of 30 m/s at 88 km and a minimum with the zero velocity at 92 km. As before, it is assumed this wind shear is distributed from 80 to 100 km height.

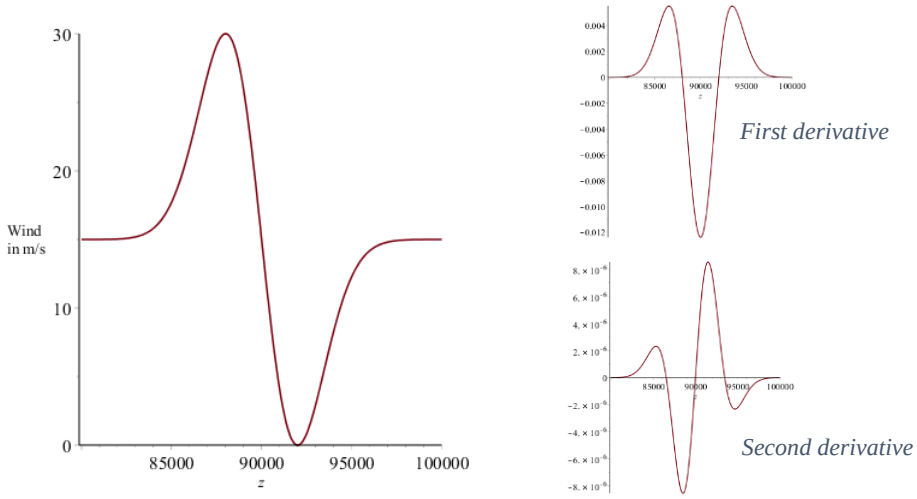

Figure 11. The background wind profile from 80 to100 km altitude with its first and second derivative profiles.

Figure 12Figure 13 plot the square of vertical wavenumber for a gravity wave with 5 min period propagating in the same direction as the wind represented by Eq. (17) . For shorter gravity waves with $\lambda \leq 25\ km$ and except over altitudes ranging from 91 to 93 km, both the TG relation and Eq. (15) predict positive m^2 with almost identical vertical wavelengths. However, for longer horizontal waves the discrepancy between two figures becomes evident as the Boussinesq approximation is no longer valid.

The main reason that our equation does not yield ducting region in heights between 91 and 93 km is because the second derivative of the background wind profile has an extremum in this region. This term in combination with the extremum in the first derivative of the background wind creates evanescent conditions for gravity waves with all horizontal wavelength. Again, because of the dominance of the second derivative term of the background wind in Eq. (15), to a good approximation one can neglect the acoustic waves term and the term with first derivative of wind velocity.

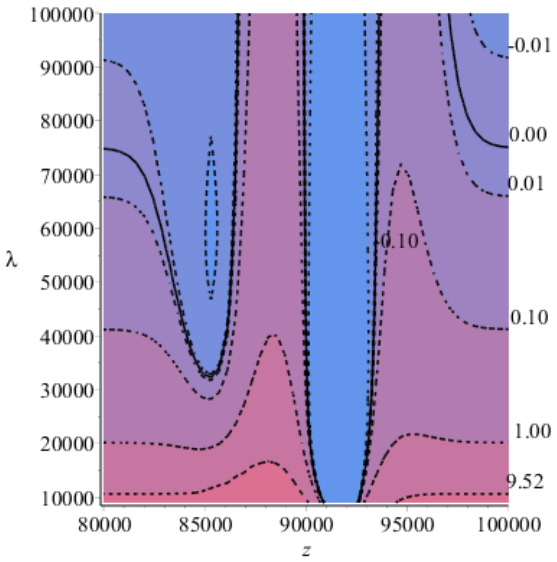

Figure 12. Vertical wavenumber square obtained for a gravity wave with 5 min period and horizontal wavelength range from 10 to 100 km propagating in an isothermal atmosphere from 80 to 100 km altitude. The m^2 values must be multiplied by 10^{-7}.

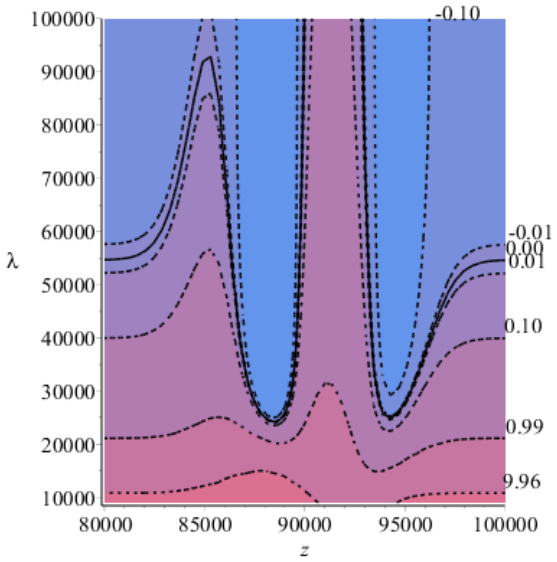

Figure 13. Vertical wavenumber square obtained by TG relation for a gravity wave with 5 min period and horizontal wavelength range from 10 to 100 km propagating in an isothermal atmosphere from 80 to 100 km altitude. The m^2 values must be multiplied by 10^{-7}.

For gravity waves with horizontal wavelength between 35 and 75 km, Eq. (15) predicts ducting conditions in the region where a maximum wind exists (from about 86 to 90 km) and evanescent conditions above and below this region. Eq. (15) predicts positive m^2 with a value from 10×10^{-7} to 0.1×10^{-7} in altitudes within about 2 km of the location of the maximum of the wind peak, complex m in the height above and below the wind peak (namely $z < 86$ km and $z > 90$ km) and real m the tails if the wind profile. The wind peak interacts with the acoustic-gravity waves to cause total reflection and horizontal ducting of the waves. Like before, the peak in the background wind serves the wave energy in this region and allows to carry wave system over great horizontal distance without significant leakage. In comparison, for waves with horizontal wavelengths from 25 to 55 km, the TG relation predicts that the these waves are evanescent.

In the following figures, the contours of m^2 for gravity waves with periods of 10, 20 and 30 min are plotted. Again, on the same scale as before, the main differences are he distances between the contours which increases significantly to support waves with larger horizontal scales.

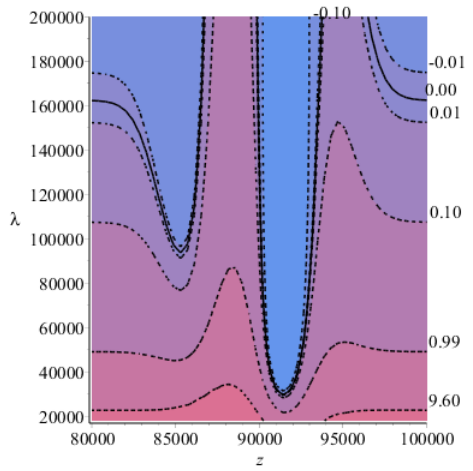

Figure 14. Vertical wavenumber square obtained for a gravity wave with 10 min period.

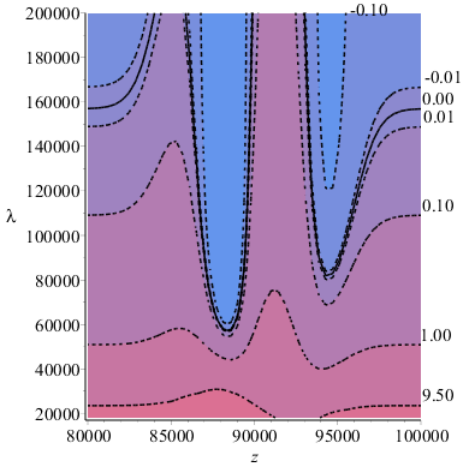

Figure 15. Vertical wavenumber square obtained by TG relation for a gravity wave with 10 min period.

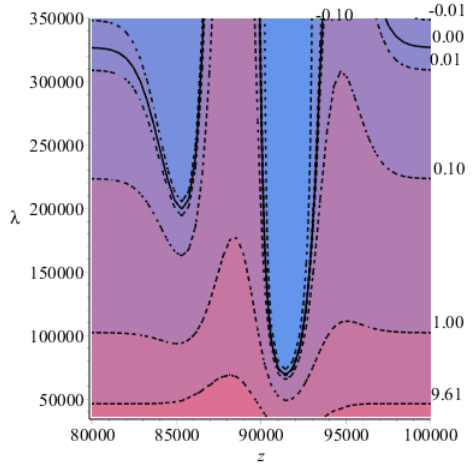

Figure 16. Vertical wavenumber square obtained for a gravity wave with 20 min period.

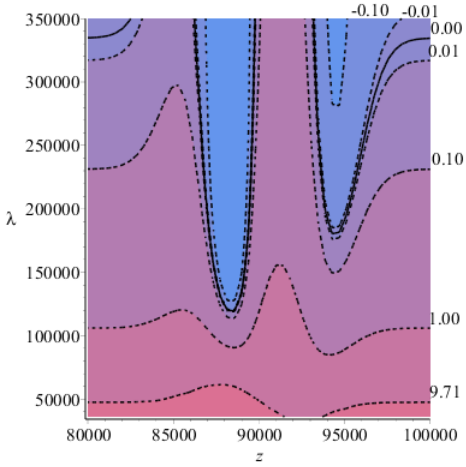

Figure 17. Vertical wavenumber square obtained by TG relation for a gravity wave with 20 min period.

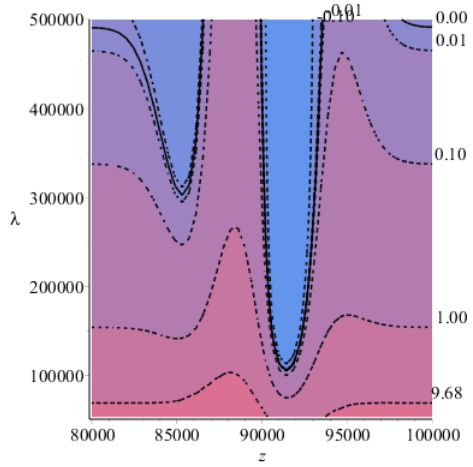

Figure 18. Vertical wavenumber square obtained for a gravity wave with 30 min period.

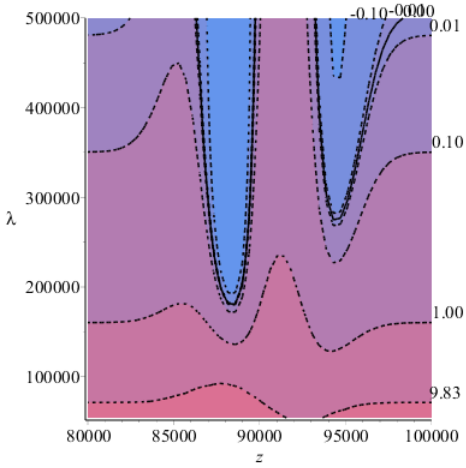

Figure 19. Vertical wavenumber square obtained by TG relation for a gravity wave with 30 min period.

3.3 Background wind with reversal derivative of Gaussian profile

Finally, we consider a gravity wave propagating in both same and opposite direction to the wind for the same distribution expressed by Eq. (17) but with the values of $U_0 = 0$, $\alpha = 10^5$, $z_0 = 90\ km$ and $\sigma = 2\ km$. This function with the given values provides a maximum in the wind velocity of $30\ m/s$ at $88\ km$ and a minimum velocity of $-30\ m/s$ at $92\ km$. The negative values in the velocity profile indicate that the background wind is moving opposite to the wave propagation direction. It is again assumed this wind duct is distributed from 80 to 100 km altitude.

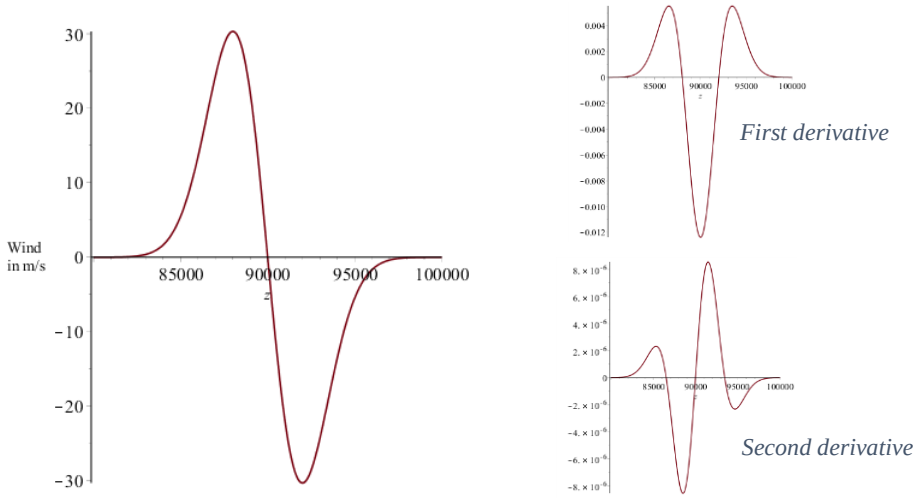

Figure 20. The background wind profile from 80 to100 km altitude with its first and second derivative profiles.

Figure 21Figure 22 represent the contour plots for m^2 for a gravity wave with 10 min period with a background wind profile as shown in Figure 20. Again, for shorter gravity waves and except in altitudes between 90 to 94 km, both the TG relation and Eq. (15) predict real m with almost identical vertical wavelengths. This is as expected as the Boussinesq approximation is valid.

For larger horizontal wavelength gravity waves, m^2 obtained by the TG relation follows well the second derivative of wind profiles. However, m^2 from Eq. (15) follows closely the opposite to the second derivative of wind profiles. This term in combination with an extremum in the first derivative of the background wind at 90 km indicates evanescent conditions for any gravity waves for all horizontal wavelength at altitudes above the critical altitude of the wind distribution (90 km) to about 94 km. Our solution shows a ducting region where the wind speed is approaching a maximum, and on either side of this region where the wind speed decreases in value, it predicts evanescent gravity waves. The smallest value of m^2 occurs at the altitudes where the wind speed has its minimum value.

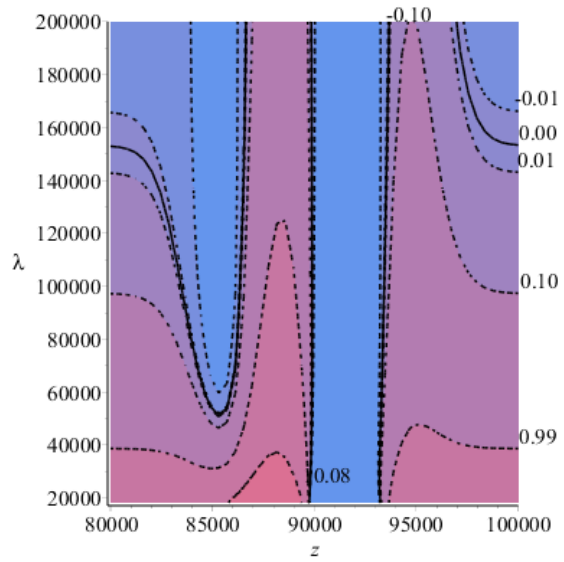

Figure 21. Vertical wavenumber square obtained for a gravity wave with 10 min period and horizontal wavelength range from 10 to 100 km propagating in an isothermal atmosphere from 80 to 100 km altitude. The m^2 values must be multiplied by 10^{-7}.

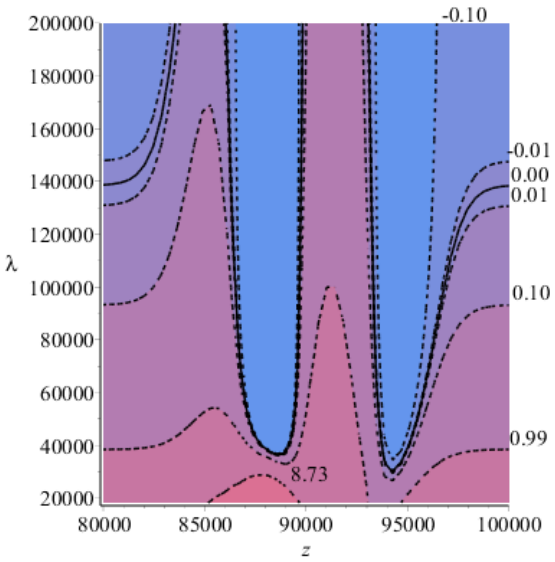

Figure 22. Vertical wavenumber square obtained by TG relation for a gravity wave with 10 min period and horizontal wavelength range from 10 to 100 km propagating in an isothermal atmosphere from 80 to 100 km altitude. The m^2 values must be multiplied by 10^{-7}.

Except for altitudes of the tails of the wind profile, the vertical wavenumber squared attained by the TG relation and by Eq. (15) are opposite in sign. One gives real m while the other one gives complex m for the same wave at the same altitude. Our equation predicts that the peak in the background wind serves the wave energy. These are all in contrast with the solution for m^2 predicted by TG relation. The conditions for ducting is found to be quite different from the TG relation.

One interesting experimental example is the gravity waves captured by Advanced Mesospheric Temperature Mapper (AMTM) from Bear Lake Observatory, UT on July 28 of 2015. The AMTM is a ground-based infrared imaging system that measures selected emission lines in the mesospheric Hydroxyl (OH) airglow emission in order to create intensity and temperature maps around $88 \pm 5\ km$ altitude. It provides high spectral sensitivity over a large 120° field of view and covers about 150×120 km^2 area of the mesosphere/mesopause. The atmospheric wind is recorded by Lidar at Utah State University, UT. The Lidar provides the continuous atmospheric wind and it's propagation direction from 82 to 98 km altitude with $\pm5\ m/s$ uncertainty. Both the AMTM and the Lidar are looking in the same volume of sky and thus provide realistic atmospheric properties for the wave propagation through the mesosphere/mesopause.

The AMTM data on July 29 of 2015 shows a ducted gravity wave with a nearly constant horizontal wavelength of $18 \pm 2\ km$. The wave phase speed is gradually increasing as it propagates initially with the period is $12 \pm 2\ min$ and later with the period of $7 \pm 2\ min$. The wave is propagating horizontally in the direction of $150°$ from North (i.e. Southeastward) continuously from 4:00 to 9:00 UT (see Figure 23). Then, the waves suddenly disappear. The hourly averaged wind recorded by Lidar shows the change of the wind profile in the wave propagation direction. The background wind gets a new profile like a negative Gaussian

distribution with a minimum wind peak of $-45 \pm 5\ m/s$ at $87 \pm 3\ km$ altitude. As explained before, the new equation predicts that the minimum of the wind speed creates the evanescent conditions for the gravity waves however, the TG relation predicts the propagation conditions in these regions.

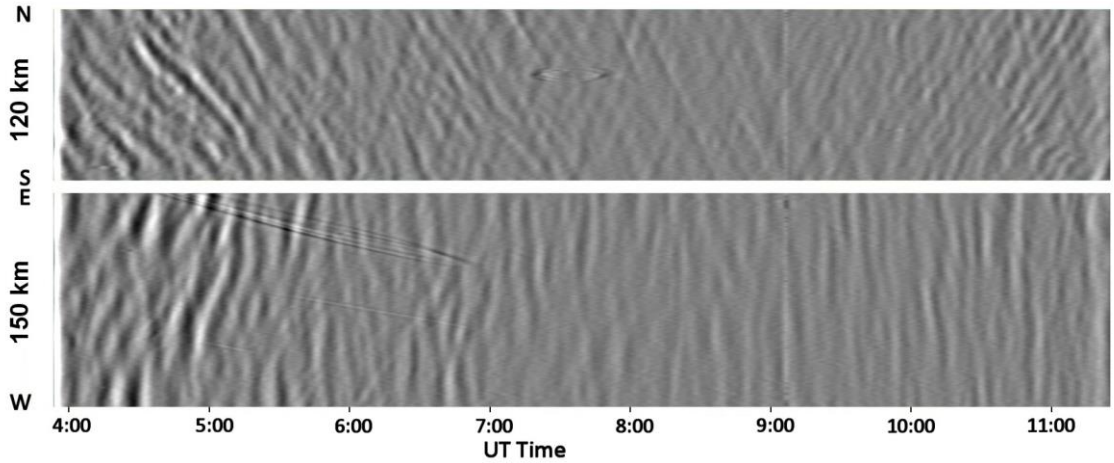

Figure 23. The AMTM data on July 28 of 2015 over Bear Lake Observatory, UT. The Figure presents a ducted gravity wave propagating horizontally in altitude of $87 \pm 5\ km$ *with a nearly constant horizontal wavelength of* $20 \pm 5\ km$ *and period of* $12 \pm 2\ min$*. The wave is propagating in the direction of* $150°$ *from North (namely toward Southeast) continuously from 4:00 to 8:00 UT and then suddenly disappears.*

4 Acoustic-gravity waves dispersion relation

Observational studies of gravity waves in the upper atmosphere often report that their horizontal propagation is opposite, or perpendicular to the background wind direction. The wave solution with the form of $w_1(x,z,t) = \widetilde{w}_1(z) \cdot \Omega \cdot e^{i(kx-\omega t)+\frac{z}{2H_s}}$ indicates that the wave amplitude is proportional to the intrinsic frequency Ω, or the term $k(c_p - u_0)$. This means the amplitude of waves moving opposite to the wind direction should increase. Indeed, high intrinsic frequency waves exhibit larger amplitude to the vertical motions. Therefore, these waves are free from severe reflection and continue to grow and propagate vertically as long as they progress in a different direction with respect to prevailing winds. The waves propagating in the same wind direction are more likely to decrease in amplitudes and finally become evanescent or be reflected by the winds. This could be an alternative explanation to the directional filtering of atmospheric waves as initially discussed by Hines and Reddy [Hines and Reddy, 1967] that, if the waves that reach the ionosphere are detected there as drifts, they would then exhibit preferred directions of motion that could be interpreted erroneously as preferred direction of the local ionospheric winds. Therefore, the waves moving opposite to the wind gain momentum from background flow while moving in the same wind direction deliver momentum to the background flow. Clearly, the waves moving perpendicular to the wind are unaffected by the background flow.

Using Eq. (15), the well-set form of the acoustic-gravity wave equation for a compressible atmosphere with non-uniform wind velocity can be rewritten as:

$$\frac{d^2\widetilde{w}_1}{dz^2} + \left[\frac{k^2N^2}{\Omega^2} + \frac{\Omega^2}{c_s^2} + \frac{d^2}{dz^2}ln\Omega - \frac{1}{4H_s^2} - k^2\right]\widetilde{w}_1 = 0 \tag{18}$$

Where the intrinsic frequency $\Omega = \omega - u_0(z)k$ is a function of z therefore, $\frac{d\Omega}{dz} = -k\frac{du_0}{dz}$, $\frac{d^2\Omega}{dz^2} = -k\frac{d^2u_0}{dz^2}$ and $\frac{d^2}{dz^2}ln\Omega = \frac{d^2\Omega}{dz^2}\frac{d}{d\Omega}ln\Omega + \left(\frac{d\Omega}{dz}\right)^2\frac{d^2}{d\Omega^2}ln\Omega$. The only difference in the wave equation when background wind in added to the governing equations is the term with the second derivative of $ln\Omega$. Indeed, this term contains the first and second derivatives of wind velocity and is only a function of height.

In a stratified atmosphere where the undisturbed density ρ_0 and other properties vary with the vertical coordinate z, it is only the z-component of wavenumber m that can vary with altitude. The horizontal wavenumber k and frequency ω remain constant. Therefore, it is not possible to obtain an exact solution to Eq. (18)(18) unless all the atmospheric terms inside the bracket take a general form of z. Much, however, can be found out about wave-like solutions to the equation from the *local* dispersion relationship where m becomes locally constant. Accordingly, the dispersion relationship for acoustic-gravity waves with a plane-wave form solution in the z direction, e.g. $\widetilde{w}_1(z) = \bar{w}e^{imz}$, becomes:

$$c_s^{-2}\Omega^4 - \left(m^2 + k^2 + \frac{1}{4H_s^2} - \frac{d^2}{dz^2}ln\Omega\right)\Omega^2 + k^2N^2 = 0 \tag{19}$$

Where the vertical wavenumber m is purely real for propagating waves and imaginary for evanescent waves. Therefore, the dispersion relation for pure gravity waves, under asymptotic limit, reduces to:

$$\Omega(z) \approx -\frac{k}{2\mathrm{K}^2}\frac{d^2u_0}{dz^2}\left[1 \pm \left(1 + \frac{\frac{g\kappa}{H_s} - \left(\frac{du_0}{dz}\right)^2}{\left(\frac{1}{2\mathrm{K}}\frac{d^2u_0}{dz^2}\right)^2}\right)^{1/2}\right] \tag{20}$$

Where $\mathrm{K}^2 = m^2 + k^2 + \frac{1}{4H_s^2}$. This equation in a stationary atmosphere gives the known dispersion relation of $\omega^2 \approx \frac{k^2N^2}{\mathrm{K}^2}$.

5 Conclusion

A modified form for the acoustic-gravity wave equation and its dispersion relationships for a compressible and non-stationary atmosphere in hydrostatic balance are presented. These solutions are achieved without the use of standard approximations, as has been the practice in past studies. It is shown that the only difference in the wave equation with and without a non-uniform wind field is a term with a second derivative of $ln\Omega$. It is also presented that the wave solution introduces the intrinsic frequency in the amplitude of the vertical velocity which may play a significant role in directional filtering of atmospheric waves in a realistic atmosphere with strong and highly variable winds. These new solutions may be particularly important for improved gravity wave propagation studies in the upper mesosphere and thermosphere/ionosphere regions.

The analyses based on conservation of wave action and impedance have identified the importance of intrinsic frequency in determining the transport of energy by gravity waves. The role of intrinsic frequency in changing the relative amplitudes of vertical and horizontal fluid motions and thus controlling the wave momentum and energy flux indeed, appears in a wide

range of literature in different contexts. The analysis presented here derives a new solution and further identifies potentially important role of Ω in supporting the amplitude growth for the waves propagate opposite to the wind direction.

The new wave equation introduced here is an important improvement to the well-known Taylor-Goldstein equation, the starting point for most recent analyses of the effects of wind shear on gravity waves. Three different background wind profiles are simulated. It is shown that our equation presents a ducting region where the wind speed is approaching a maximum, and in the either side this region where the wind speed is decreasing in value, it predicts evanescent gravity waves. Indeed, our equation predicts that the peak in the background wind serves the wave energy and allows to carry wave system over great horizontal distance without significant leakage. It also predicts the evanescent region where the wind speed is approaching a minimum. The conditions for ducting is found to be quite different from the TG relation.

Acknowledgments and Data

We kindly acknowledge Dr. T. Yuan from Center for Atmospheric and Space Science (CASS) for providing the observational Lidar data used to model the realistic wind profiles and Dr. P. -D Patutet also from CASS for his help in the analyses of coincident AMTM gravity wave data. We also thank Dr. L. Scherliess and Dr. C. Torre from Department of Physics at Utah State University for their valuable help in cross-checking our mathematical analyses. This research was supported in part under NFS grant No. 1042227 and 1338666. The Lidar data were obtained as part of the NSF grant No. 1135882.

References

Booker, John R., and Francis P. Bretherton (1967), The critical layer for internal gravity waves in a shear flow, Journal of Fluid Mechanics, vol. 27, pp. 513-539

Bretherton, F. P. (1966), The propagation of groups of internal gravity waves in a shear flow, Quarterly Journal of Royal Meteorological Society, vol. 92, pp. 466–480

Chimonas, G. (1997), Waves and the Middle Atmosphere Wind Irregularities, Journal of Atmospheric Sciences, vol. 54, pp. 2115–2128

Chimonas, G. (2002), On internal gravity waves associated with the stable boundary layer, Boundary-Layer Meteorology, vol. 102, pp. 139–155

Chimonas, G., and C. O. Hines (1986), Doppler Ducting of Atmospheric Gravity Waves, Journal of Geophysical Research, vol. 91, no. D1 pp. 1219–1230

Drazin, P. G. (2002), Introduction to Hydrodynamic Stability, Cambridge University Press

Fua, D., F. Einaudi, and D. P. Lalas (1976), The stability analysis of an inflection-free velocity profile and its applications to the night-time boundary layer in the atmosphere, Boundary-Layer Meteorology, Vol. 10, no. 1, pp.35–54

Fritts, D. C. and M. J. Alexander (2003), Gravity wave dynamics and effects in the middle atmosphere, Reviews of Geophysics, vol. 41, no.1, pp. 1–59

Fua, D., and F. Einaudi (1984), On the effects of dissipation on shear instabilities in the stable atmospheric boundary layer, Journal of Atmospheric Sciences, vol. 41, pp. 888–900

Garcia, R. R., and S. Solomon (1985), The effect of breaking gravity waves on the dynamical and chemical composition of the mesosphere and lower thermosphere, Journal of Geophysical Research, vol. 90, pp. 3850–3868

Garratt, J. R. (1992), The Atmospheric Boundary Layer, Cambridge University Press

Goldstein, S. (1931), On the Stability of Superposed Streams of Fluids of Different Densities, Proceeding of the Royal Society of London A, vol. 132, pp. 524-548

Gossard, E. E., and W. H. Hooke (1975), Waves in the Atmosphere: Atmospheric Infrasound and Gravity Waves, Their Generation and Propagation, Elsevier, New York

Hazel, Philip (1972), Numerical studies of the stability of inviscid stratified shear flows, Journal of Fluid Mechanics, vol. 51, pp. 39-61

Hines, C. O., (1960), Internal Atmospheric Gravity Waves at Ionospheric Heights, Canadian Journal of Physics, vol. 88, pp. 1441-1481

Hines, C. O., and C. A. Reddy (1967), On the Propagation of Atmospheric Gravity Waves through Regions of Wind Shear, Journal of Geophysics Research, vol. 72, no. 3, pp. 1015-1034

Holton, J. R. (1982), The role of gravity wave induced drag and diffusion in the momentum budget of the mesosphere, Journal of Atmospheric Sciences, vol. 39, pp. 791–799

Hocke, K. and K. Schlegel (1996), A review of atmospheric gravity waves and travelling ionospheric disturbances: 1982-1995, Ann. Geophys., vol. 14, pp. 917–940

Isler, R. J., M. J. Taylor, and D. C. Fritts, Observational evidence of wave ducting and evanescence in the mesosphere, Journal of Geophysical Research, vol. 102, no. D22, pp. 301–313

Jones, Walter L. (1968), Reflection and stability of waves in stably stratified fluids with shear flow: a numerical study, Journal of Fluid Mechanics, vol. 34, pp. 609-624

Lalas, D. P., and F. Einaudi, (1976), On the characteristics of gravity waves generated by atmospheric shear layers, Journal of Atmospheric Sciences, vol. 33, pp. 1248–1259

Levich, V. (1962), Physicochemical Hydrodynamics, Prentice-Hall International, Inc. New Jersey

Lighthill, M. J. (1978), Waves in Fluids, Cambridge University Press, UK

Liller, W., and F. L. Whipple (1954), High-altitude winds by meteor-train photography, Rocket Exploration of the Upper Atmosphere, vol. 1, pp. 112-130

Lindzen, R. S. (1973), Wave-mean flow interactions in the upper atmosphere, Boundary Layer Meteorology, vol. 4, pp. 327–343

Lindzen, R. S. (1981), Turbulence and stress owing to gravity wave and tidal breakdown, Journal of Geophysical Research, vol. 86, pp. 9707–9714

Lindzen, R. S. and K. K. Tung (1976), Banded Convective Activity and Ducted Gravity Waves, Monthly Weather Review, vol. 104, pp. 1602-1617

Nappo, C. J. (2014), An Introduction to Atmospheric Gravity Waves, 2ed edition, International Geophysics Series, vol. 102, Academic Press, Amsterdam

Pautet, P.-D., M. J. Taylor, A. Z. Liu, and G. R. Swenson (2005), Climatology of short-period gravity waves observed over northern Australia during the Darwin are wave experiment (DAWEX) and their dominant source regions, Journal of Geophysical Research, vol. 110, no. D03S90, pp. 1-13

Sutherland, B. R., C. P. Caulfield, and W.R. Peltier (1994), Internal gravity wave generation and hydrodynamic instability, Journal of Atmospheric Sciences, vol. 51, pp. 3261–3280

Taylor, G. I. (1931), Effect of Variation in Density on the Stability of Superposed Streams of Fluid, Proceeding of the Royal Society of London A, vol. 201, pp: 499-523

Teixeira, Miguel A. C., Pedro M. A. Miranda, and Maria Antónia Valente (2004), An Analytical Model of Mountain Wave Drag for Wind Profiles with Shear and Curvature, Journal of Atmospheric Sciences, vol. 61, pp. 1040–1054

Turner, J. S. (1973), Buoyancy Effects in Fluids, Cambridge University Press

Vadas, Sharon L. (2007), Horizontal and vertical propagation, and dissipation of gravity waves in the thermosphere from lower atmospheric and thermospheric sources, Journal of Geophysical Research, vol. 112, no. A06305, pp. 1-23

Vadas, Sharon L., and D. C. Fritts (2005), Thermospheric responses to gravity waves: Influences of increasing viscosity and thermal diffusivity, Journal of Geophysical Research, vol. 110, no. D15103, pp. 1-16

Vallis, Geoffrey K. (2006), Atmospheric and Oceanic Fluid Dynamics: Fundamentals and Large-scale Circulation, Cambridge University Press, UK